

3. F. A. Edwards, A. Konnerth, B. Sakmann, *J. Physiol. London* **430**, 213 (1990).
4. S. W. Kuffler and D. Yoshikami, *ibid.* **251**, 465 (1975).
5. F. Edwards, *Nature* **350**, 271 (1991).
6. F. R. Edwards, S. J. Redman, B. Walmsley, *J. Physiol. London* **259**, 689 (1976); J. J. B. Jack, S. J. Redman, K. Wong, *ibid.* **321**, 65 (1981).
7. H. Korn and D. S. Faber, *Trends Neurosci.* **14**, 439 (1991).
8. H. Korn, A. Mallet, A. Triller, D. S. Faber, *J. Neurophysiol.* **48**, 679 (1982).
9. H. Korn, Y. Burnod, D. S. Faber, *Proc. Natl. Acad. Sci. U.S.A.* **84**, 5981 (1987); H. Korn and D. S. Faber, *J. Neurophysiol.* **63**, 198 (1990).
10. N. Roper, R. Miles, H. Korn, *J. Physiol. London* **428**, 287 (1990).
11. J. M. Bekkers, G. B. Richerson, C. F. Stevens, *Proc. Natl. Acad. Sci. U.S.A.* **87**, 5359 (1990).
12. J. M. Bekkers and C. F. Stevens, *Nature* **346**, 724 (1990); R. Malinow and R. W. Tsien, *ibid.*, p. 859; A. Margaroli and R. Tsien, *ibid.* **357**, 134 (1992).
13. T. D. Foster and B. L. McNaughton, *Hippocampus* **1**, 79 (1991); D. M. Kullman and R. A. Nicoll, *Nature* **357**, 240 (1992).
14. T. Manabe, P. Renner, R. A. Nicoll, *Nature* **355**, 50 (1992).
15. H. Korn, C. Fassnacht, D. S. Faber, *ibid.* **350**, 282 (1991); D. S. Faber and H. Korn, *Biophys. J.* **60**, 1288 (1991).
16. A. Triller and H. Korn, *J. Neurophysiol.* **48**, 7081 (1982); our results are not changed by modification of total contact area, unless the receptor-free annulus is reduced drastically, producing a smaller q .
17. The average distance moved is obtained from the Einstein equation, with a Gaussian distribution function. See T. M. Bartol, Jr., B. R. Land, E. E. Salpeter, and M. M. Salpeter [*Biophys. J.* **59**, 1290 (1991)] for a detailed description of Monte Carlo simulations of miniature endplate currents, including methods for validating diffusion. The finer grid size used in that study increases computational time more than tenfold without altering q or kinetics.
18. The estimated number, n , of binding sites per glycine receptor is in the range of 2 to 3 [J. Diamond and S. Roper, *J. Physiol. London* **232**, 113 (1973); H. Akagi and R. Miledi, *Science* **242**, 270 (1988)]. In comparison with $n = 2$, responses simulated with $n = 3$ are 3 to 5% smaller at their peak, and their rise and half-decay times are 15 to 25% faster than those of the $n = 2$ responses. The possibility that the glycine receptor may have multiple open states, as in mouse spinal neurons [R. E. Twyman and R. L. MacDonald, *J. Physiol. London* **435**, 303 (1991)], was not incorporated into the model.
19. Transition probabilities are calculated from the matrix:

$$\begin{array}{c}
 R \text{ (free)} \quad AR \text{ (single bound)} \\
 \begin{array}{c} R \\ AR \\ A_2R \\ A_2R^* \end{array} \left[\begin{array}{cc} 1 - k_{+1}a\Delta t & k_{+1}a\Delta t \\ k_{-1}\Delta t & 1 - (k_{-1} + k_{+2}a)\Delta t \\ 0 & k_{-2}\Delta t \\ 0 & 0 \end{array} \right. \\
 A_2R \text{ (double)} \quad A_2R^* \text{ (open)} \\
 \begin{array}{c} R \\ AR \\ A_2R \\ A_2R^* \end{array} \left. \begin{array}{cc} 0 & 0 \\ k_{+2}a\Delta t & 0 \\ 1 - (k_{-2} + \beta)\Delta t & \beta\Delta t \\ \alpha\Delta t & 1 - \alpha\Delta t \end{array} \right]
 \end{array}$$

where the transitions are from the state in the first column to the state in the top row, a is the transmitter concentration in the "cell" above the receptor, and probabilities in each row sum to 1.

20. D. S. Faber and H. Korn, *J. Neurophysiol.* **60**, 1982 (1988).
21. ———, *Science* **208**, 612 (1980), *J. Neurophysiol.* **48**, 654 (1982).
22. A. B. Young and S. H. Snyder, *Proc. Natl. Acad. Sci. U.S.A.* **70**, 2832 (1973).
23. Setting $k_{-2} = 10 k_{-1}$ treats the two binding steps as nonequivalent, with the affinity higher for the first one. This relation applies to the nicotinic acetylcholine receptor [P. Blount and J. P. Merlie, *Neuron* **3**, 349 (1989)]; glycinergic responses simulated with equivalent binding give the same results presented here.
24. D. S. Faber and H. Korn, *Proc. Natl. Acad. Sci. U.S.A.* **85**, 8708 (1988).
25. M. Solodkin *et al.*, *J. Neurophysiol.* **65**, 927 (1991).
26. P. Legendre and H. Korn, *Soc. Neurosci. Abstr.* **18**, 1357 (1992).
27. Because the responses are not saturated, an increase in the background transmitter concentration in the synaptic cleft, for example, by lateral diffusion from adjacent synapses (10) could still enhance q . This effect results when one primes the receptors and increases the probability of channel opening.
28. G. Vrensen *et al.*, *Brain Res.* **184**, 23 (1980).
29. R. Angus Silver, S. F. Traynelis, S. G. Cull-Candy, *Nature* **355**, 163 (1992).
30. F. J. Sigworth, *J. Physiol. London* **307**, 97 (1980).
31. H. P. C. Robinson, Y. Sahara, N. Kawai, *Biophys. J.* **59**, 295 (1991).
32. H. C. Fertuck and M. M. Salpeter, *J. Cell Biol.* **69**, 144 (1976).
33. H. C. Hartzell, S. W. Kuffler, D. Yoshikami, *J. Physiol. London* **251**, 427 (1975).
34. T. Seitanidou, A. Triller, H. Korn, *J. Neurosci.* **8**, 4319 (1988).
35. G. Lynch and M. Baudry, *Science* **224**, 1057 (1984), J. A. Kauer, R. C. Malenka, R. A. Nicoll, *Neuron* **1**, 911 (1988).
36. Supported in part by grants from the NIH (NS 21848) and Direction des Recherches, Etudes et Techniques (92/058).

9 June 1992, accepted 8 September 1992

The Time Course of Glutamate in the Synaptic Cleft

John D. Clements,* Robin A. J. Lester,† Gang Tong, Craig E. Jahr, Gary L. Westbrook

The peak concentration and rate of clearance of neurotransmitter from the synaptic cleft are important determinants of synaptic function, yet the neurotransmitter concentration time course is unknown at synapses in the brain. The time course of free glutamate in the cleft was estimated by kinetic analysis of the displacement of a rapidly dissociating competitive antagonist from *N*-methyl-D-aspartate (NMDA) receptors during synaptic transmission. Glutamate peaked at 1.1 millimolar and decayed with a time constant of 1.2 milliseconds at cultured hippocampal synapses. This time course implies that transmitter saturates postsynaptic NMDA receptors. However, glutamate dissociates much more rapidly from α -amino-3-hydroxy-5-methyl-4-isoxazolepropionic acid (AMPA) receptors. Thus, the time course of free glutamate predicts that dissociation contributes to the decay of the AMPA receptor-mediated postsynaptic current.

The time course of neurotransmitter in the synaptic cleft has not been directly measured. At the frog neuromuscular junction, the time course of free acetylcholine (ACh) has been estimated from the shape of miniature end-plate currents (1) and is brief, principally due to rapid hydrolysis of ACh by acetylcholinesterase (2). Central glutamate-mediated synapses differ from the neuromuscular junction in that transmitter clearance depends on diffusion and reuptake rather than enzymatic breakdown (3). Central synapses also differ in their morphology (4, 5) and quantal characteristics of transmitter release (6, 7). The time course of free glutamate at hippocampal synapses must account for both fast and slow excitatory postsynaptic currents (EPSCs)

mediated by co-localized AMPA and NMDA receptors (8). Although transmitter clearance is not the rate-limiting factor for the NMDA receptor-mediated EPSC (9), rapid desensitization of AMPA receptors (10) could mask the persistence of free transmitter. A detailed understanding of transmission at these synapses requires knowledge of the time course of glutamate in the cleft.

We estimated the concentration time course of free glutamate in the cleft by measuring the nonequilibrium reduction of NMDA receptor-mediated EPSCs produced by the rapidly dissociating antagonist D-aminoadipate (D-AA) (11). This antagonist is expected to reduce transmission by an amount proportional to its equilibrium occupancy of the postsynaptic receptors, less an amount due to glutamate displacement of D-AA on some receptors. The longer that transmitter is present, the more D-AA will be replaced by glutamate. This process provides a means to estimate the peak concentration and duration of transmitter at the postsynaptic membrane. To determine the transmitter time course by this method, several parameters must be known. These include the number of agonist and antagonist binding sites per recep-

J. D. Clements and R. A. J. Lester, Vollum Institute, Oregon Health Sciences University, Portland, OR 97201.

G. Tong and C. E. Jahr, Vollum Institute and Department of Cell Biology and Anatomy, Oregon Health Sciences University, Portland, OR 97201

G. L. Westbrook, Vollum Institute and Department of Neurology, Oregon Health Sciences University, Portland, OR 97201.

*To whom correspondence should be addressed

†Present address: Department of Molecular Physiology and Biophysics, Baylor College of Medicine, One Baylor Plaza, Houston, TX 77030

tor, the equilibrium dissociation constants (K_d 's), and binding and unbinding rates of glutamate and D-AA.

Parallel experiments were conducted with the high-affinity NMDA-receptor antagonist D-carboxypiperazin-propyl-phosphonic acid (D-CPP), which has relatively slow binding and unbinding rates (12). Because of these slow rates, its receptor occupancy should not deviate significantly from equilibrium, on the assumption that transmitter is cleared within 10 to 20 ms. In whole-cell recording from cultured hippocampal neurons (13), long pulses (5 s) of D-AA (100 μ M) or D-CPP (1 μ M) in the continuous presence of NMDA (10 μ M) were approximately equipotent (74 \pm 3% inhibition by D-AA and 71 \pm 3% inhibition by D-CPP, mean \pm SEM, $n = 4$) (Fig. 1A). The block and recovery rates were much slower for D-CPP, reflecting its slow binding and unbinding rates. This result suggests that D-AA and D-CPP at the above concentrations should be equipotent in blocking synaptic transmission only if transmitter is present for a period much less than the unbinding rate of D-AA. However, they were not equipotent at blocking NMDA receptor-mediated EPSCs (Fig. 1B) (14). Although D-CPP reduced EPSCs by 88 \pm 0.5% ($n = 4$), close to the block predicted if the transmitter pulse produced

no antagonist displacement (\sim 90%), D-AA reduced the same EPSCs by 78 \pm 1% ($n = 4$), much less than the predicted block and significantly less than D-CPP ($P < 0.01$, paired t test). Similar results were obtained at other D-AA and D-CPP concentrations ($n = 12$), and in every case D-AA was less effective at blocking synaptic transmission than predicted from its equilibrium block of NMDA current. These results suggest that transmitter is present in the synaptic cleft for a sufficiently long time at a sufficiently high concentration to displace some of the D-AA from the NMDA receptors. However, it is not present long enough to displace the more slowly dissociating D-CPP.

The displacement of antagonist by transmitter is affected by the stoichiometry of antagonist binding to the NMDA receptor-channel complex. There are two glutamate binding sites per NMDA channel (15, 16), but it has been suggested that there is only one "antagonist-preferring" site per channel (17). To confirm the presence of two antagonist binding sites as suggested by whole-cell studies (16), the percentage of channels that bind D-CPP was probed with a brief pulse (4 ms) of a saturating concentration of NMDA (1 mM) applied to an outside-out membrane patch (18) (Fig. 1C). Because the dissociation rate, k_{off} , for

D-CPP is slow (1.1 s^{-1}) (12), a 4-ms NMDA pulse should displace virtually no D-CPP. If only one antagonist binding site is available per channel, then 50% of the channels will be occupied at the dissociation constant, K_d . However, if two sites are available, then antagonist will bind to 75% of the channels (50% with one site and 25% with both sites occupied). Preequilibration with D-CPP at its K_d (400 nM) (12, 16) reduced the response to NMDA by 72 \pm 2% ($n = 6$) (Fig. 1C), a result consistent with two antagonist binding sites per channel. To measure the K_d of D-AA, we recorded whole-cell currents produced by NMDA (10 to 3000 μ M) under control conditions and in the presence of D-AA (20 to 1000 μ M) ($n = 16$ cells). The K_d for D-AA estimated from dose-response curve fitting (12) and dose ratio analysis ranged from 20 to 40 μ M. Thus a K_d of 30 μ M was chosen for the subsequent analysis. This is higher than the K_d estimated from displacement of [3 H]D-AP5 binding (13 μ M) (19) but consistent with an estimate from inhibition of NMDA-evoked responses in frog spinal cord (36 μ M) (20).

NMDA receptor-mediated EPSCs were recorded at a series of concentrations of D-AA and D-CPP. The inhibition of EPSCs by D-AA was compared to the dose-response curves predicted by a two-site equilibrium binding model where the transmitter pulse produces no antagonist displacement (Fig. 1D). The predicted curves used a K_d of 400 nM for D-CPP and a K_d of 30 μ M for D-AA. The inhibition of the EPSC by D-CPP is consistent with the predicted equilibrium block, but D-AA differs systematically and significantly, consistent with nonequilibrium displacement of D-AA by glutamate after synaptic release. This discrepancy could not be explained by an inaccurate estimate of the K_d for D-AA because a value of \sim 85 μ M would be necessary to fit the EPSC inhibition curve. The difference between predicted and observed inhibition curves provides the basis for estimation of the transmitter-concentration time course if the binding and unbinding rates for glutamate and D-AA are known.

Binding and unbinding rates estimated for glutamate (15) are 5 μ M $^{-1}$ s $^{-1}$ (k_{on}) and 5 s $^{-1}$ (k_{off}). To determine the binding rate of D-AA, we compared the response evoked by a very brief pulse (1 to 2 ms) of glutamate plus D-AA (both at 2 mM) to the response produced by glutamate alone (2 mM) on the same outside-out patch (Fig. 2A). Brief pulses were used to minimize the opportunity for D-AA to unbind and be replaced by glutamate. If no replacement occurs and glutamate and D-AA have identical binding rates, then 50% of the receptors will bind each drug and a response

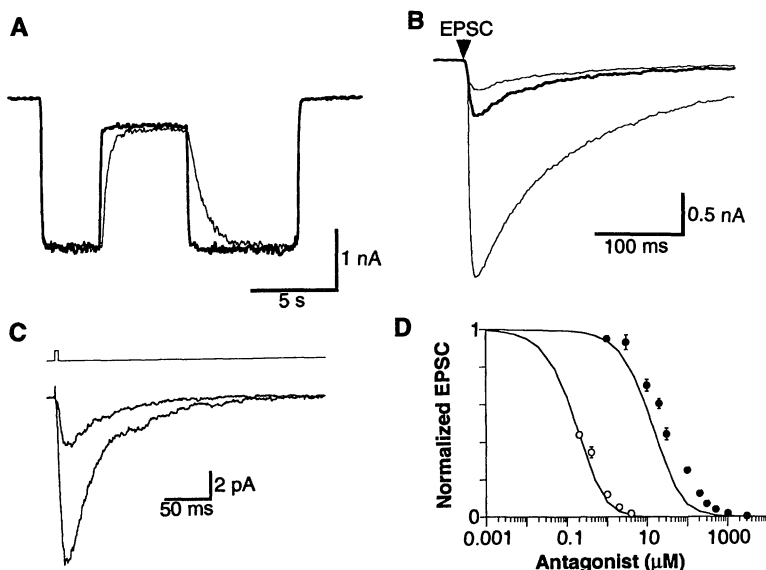


Fig. 1. (A) Equilibrium inhibition. A 15-s pulse of NMDA (10 μ M) was applied to a cultured hippocampal neuron in whole-cell voltage-clamp configuration. The competitive antagonists D-CPP (1 μ M, thin line) or D-AA (100 μ M, thick line) were applied for 5 s in the continuous presence of NMDA. (B) Nonequilibrium inhibition. NMDA receptor-mediated EPSCs were recorded between pairs of cultured hippocampal neurons under control conditions and in the presence of D-CPP (1 μ M, upper thin line) or D-AA (100 μ M, thick line); control, lower thin line. (C) The ensemble average current recorded in an outside-out patch in response to a brief pulse (5 ms) of NMDA (1 mM) under control conditions and after preequilibration with D-CPP (400 nM, smaller amplitude response); control, greater amplitude response. (D) Normalized NMDA receptor-mediated EPSC amplitude as a function of competitive antagonist concentration. Average results are shown for D-CPP (open circles) and D-AA (filled circles). The dose-response curves predicted by a two-site equilibrium binding model that assumes the transmitter pulse produced no antagonist displacement are shown, with assumed K_d 's of 400 nM for D-CPP and 30 μ M for D-AA (lines).

amplitude equal to 25% of control is expected. The measured response was only 18% of control, which implies that k_{on} is faster for D-AA than for glutamate. After correcting for the small amount of D-AA unbinding that occurs during the pulse, we calculated the D-AA binding rate at $8.1 \pm 0.5 \mu\text{M}^{-1} \text{s}^{-1}$ ($n = 21$). Measurement of the D-AA unbinding rate was conducted by the application of pulses (1 to 45 ms) of glutamate (5 mM) to outside-out patches in the continuous presence of saturating concentrations of D-AA (200 μM) (Fig. 2B). As expected, increases in glutamate pulse length reduced the effectiveness of D-AA in blocking the response. Also, preequilibration with D-AA slowed the rise of the response to glutamate pulses ≥ 10 ms. The responses to 45-ms glutamate pulses were optimally fitted with a kinetic model (21, 22). For eight patches, the D-AA unbinding rate was $160 \pm 15 \text{s}^{-1}$.

Having determined the necessary kinetic parameters, we used the reduction of synaptic transmission by D-AA to estimate the time course of glutamate in the synaptic cleft. A model incorporating binding and unbinding rates for D-AA (23) and glutamate (Fig. 3A) was used to calculate the response to a simulated synaptic pulse of glutamate. The pulse had an instantaneous rise and an exponential decay. The simulated response was also calculated for a range of D-AA concentrations. The peak glutamate concentration and the decay time constant were systematically varied until the best fit between the simulated and measured synaptic dose-response curves was reached (24). An optimal fit was obtained with a glutamate concentration that peaked at 1.1 mM and decayed with a time constant of 1.2 ms. Figure 3B shows the optimally fitted D-AA dose-response curve (dashed line) with the EPSC amplitudes from Fig. 1D (circles). The model provides an adequate fit to the

experimental observations at all D-AA concentrations. The optimal transmitter time course and the simulated NMDA receptor-mediated EPSC that it produces are shown in Fig. 3C. The 10 to 90% rise time of the simulated EPSC was 7.9 ms, virtually identical to that measured for NMDA receptor-mediated EPSCs (7.7 ms) (9).

These results provide a direct experimental estimate of the time course of glutamate in the synaptic cleft. This quantitative estimate relies on a kinetic model that incorporates several experimentally estimated affinities and rate constants. The effect of uncertainties in these parameters on the derived time course was investigated. Variation of the K_d of D-AA over the range of 20 to 40 μM resulted in almost no change in the peak concentration estimate of 1.1 mM but produced a range of decay time-constant estimates from 0.95 to 1.8 ms. We calculated confidence intervals for the two parameters by systematically setting model rate constants to upper and lower ends of the range of experimental uncertainty and reestimating the transmitter time course. The decay time constant was much more sensitive to changes in model parameters than was the peak concentration. The confidence interval estimates had peak concentration at 1.0 to 1.5 mM and the decay time constant at 0.7 to 2.0 ms.

In addition to kinetic analysis, upper and lower limits for transmitter time course parameters can be determined directly from the experimental data. For example, glutamate cannot be present in the cleft at concentrations > 1 mM for more than 100 to 200 μs because 1 mM D-AA is sufficient to block the synaptic response (Fig. 3B). It must be present at concentrations $> 100 \mu\text{M}$ for more than 1 ms because of the deviation from the equilibrium dose-response curve (Fig. 3B). The concentration cannot be greater than 50 μM for more than 5 ms,

otherwise the rise time of the synaptic current would be slowed by several milliseconds in the presence of D-AA. However, the 20 to 80% rise time was not significantly slower in 100 or 200 μM D-AA ($4.8 \pm 0.5 \text{ms}$, $n = 7$) compared to control ($4.0 \pm 0.3 \text{ms}$, $P > 0.05$, paired t test).

Our estimate of transmitter time course is compatible with the dimensions of the synaptic cleft. A synaptic vesicle at an excitatory synapse has an average diameter of 40 nm (5, 25) with an estimated glutamate concentration of 60 to 210 mM (26), and the width of the cleft is ~ 20 nm (4, 5). To dilute the contents of a single vesicle to 1 mM would require a cleft diameter of 0.4 to 0.8 μm , which is consistent with the observed range (5). The size and detailed geometry of an individual bouton should influence peak transmitter concentration and time course of clearance. Although we did not consider bouton-to-bouton variations, the estimated

Fig. 2. (A) Ensemble average current in response to brief (2 ms) pulses of glutamate alone (left, 2 mM) or glutamate plus D-AA (right, both 2 mM). The amplitude of the glutamate plus D-AA response was normalized relative to the amplitude of the glutamate response and results from 21 patches are summarized in the inset histogram. (B) Ensemble average current recorded in an outside-out patch in response to brief pulses (1 ms, top line; 2.5 ms, second line; 10 ms, third line; 45 ms, bottom line) of glutamate (5 mM) in the continuous presence of D-AA (200 μM). The response of the same patch to a 45-ms pulse of glutamate in the absence of D-AA is also shown (dots). Ensemble averages were constructed from interleaved pulse lengths to obviate the effects of rundown that occurred in some patches.

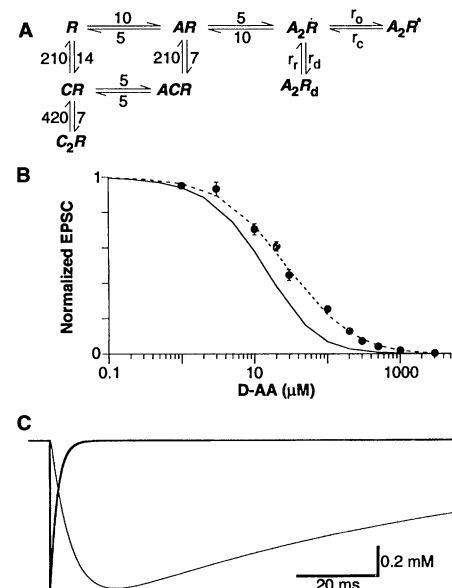
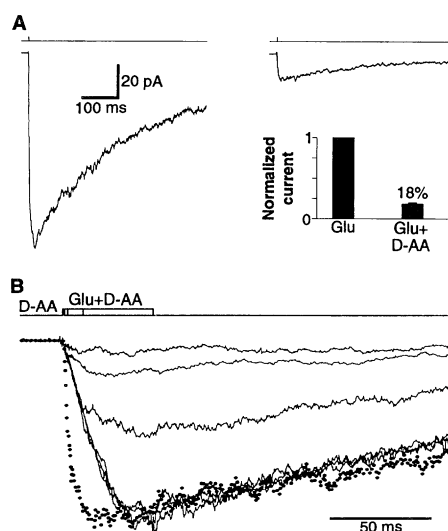


Fig. 3. (A) The reaction scheme used to model the chemical kinetic properties of the binding and unbinding of glutamate and D-AA on the NMDA receptor. Abbreviations: R , NMDA receptor; A , molecule of agonist; C , molecule of competitive antagonist; R^* , open state; R_d , desensitized state; r_o , opening rate; r_c , closing rate; r_d , desensitization rate; and r_r , resensitization rate. The binding rates ($\mu\text{M}^{-1} \text{s}^{-1}$) and unbinding rates (s^{-1}) for glutamate and D-AA are shown. (B) Normalized EPSC amplitude as a function of D-AA concentration (filled circles). The dose-response curves were predicted by a two-site equilibrium binding model for a transmitter pulse that displaces no antagonist (solid line) and for an exponentially decaying pulse of transmitter [1.1 mM peak, 1.2-ms decay time constant (dashed line)]. The K_d for D-AA was set at 30 μM . (C) The estimated transmitter concentration transient (thick line), and the simulated NMDA receptor-mediated synaptic current produced by this transient (thin line).

time course represents the average for a synapse composed of many boutons.

A simple diffusion model predicts that, after vesicle fusion, transmitter will reach the postsynaptic membrane in $<10 \mu\text{s}$ and then spread through the cleft in 50 to $100 \mu\text{s}$ (4). Almost no D-AA will dissociate in the first $100 \mu\text{s}$, so our technique is insensitive to variations in transmitter concentration during this early phase. A small region of postsynaptic receptors directly beneath the vesicle release site will be exposed to a 10- to $50\text{-}\mu\text{s}$ pulse of transmitter with a peak concentration much greater than 1 mM . However, the majority of the receptors will experience a concentration time course similar to the one estimated above. A two-dimensional infinite disk diffusion model with no diffusion barriers and negligible uptake predicts that clearance should be roughly twice as fast as the 1.2-ms time constant estimated in the present study (4). This difference suggests that diffusion away from the cleft may be restricted by neighboring structures and makes it plausible that plasmalemmal glutamate transporters could alter the transmitter time course depending on their location and density.

For both the end plate nicotinic acetylcholine receptor and the NMDA receptor, the synaptic current decay reflects channel kinetics and is much longer than the duration of free transmitter (9, 27). It has been suggested that rapid desensitization (time constant $\sim 5 \text{ ms}$) of the AMPA channel determines the decay time course of fast synaptic currents mediated by AMPA receptors (10). For this suggestion to be true, either transmitter must remain present at concentrations $>K_d$ ($\sim 250 \mu\text{M}$) for more than 5 ms or dissociation of transmitter from the AMPA receptor must be slow ($>10 \text{ ms}$). The results presented above suggest that transmitter concentration falls below $250 \mu\text{M}$ in $<2 \text{ ms}$. The low affinity of the AMPA receptor for glutamate and the rapid current decay after a brief pulse of glutamate to an outside-out patch (28) suggest a dissociation rate in the range of 1 to 5 ms. Together, these results suggest that transmitter dissociation as well as desensitization determines the decay of the fast EPSC.

The receptor occupancy (degree of saturation) for postsynaptic NMDA receptors after synaptic release can be estimated from knowledge of transmitter time course and rates of binding and unbinding. Our results imply that 97% of NMDA channels bind two molecules of glutamate after release from a single vesicle. The glutamate binding rate and stoichiometry at AMPA receptors are not known, but their K_d at $250 \mu\text{M}$ (29) is much higher than that for NMDA receptors. Only 60% of AMPA channels would bind two molecules of glutamate after synaptic release, with an assumed similar binding rate and stoichiometry to NMDA recep-

tors. Thus, variations in vesicle size, multivesicular release, or changes in transmitter clearance could alter receptor occupancy, leading to changes in synaptic efficacy. Such behavior has been observed at the neuromuscular junction, particularly when the transmitter time course is prolonged by inhibition of acetylcholinesterase (30).

REFERENCES AND NOTES

- B. Katz and R. Miledi, *J. Physiol. London* **231**, 549 (1973); P. W. Gage and R. N. McBurney, *ibid.* **244**, 385 (1975); B. R. Land, W. V. Harris, E. E. Salpeter, M. M. Salpeter, *Proc. Natl. Acad. Sci. U.S.A.* **81**, 1594 (1984); T. M. Bartol, Jr., B. R. Land, E. E. Salpeter, M. M. Salpeter, *Biophys. J.* **59**, 1290 (1991).
- M. M. Salpeter, in *The Vertebrate Neuromuscular Junction*, M. M. Salpeter, Ed. (Liss, New York, 1987), p. 1.
- J. C. Watkins and R. H. Evans, *Annu. Rev. Pharmacol. Toxicol.* **21**, 165 (1981).
- J. C. Eccles and J. C. Jaeger, *Proc. R. Soc. London Ser. B* **148**, 38 (1958).
- K. M. Harris and D. M. Landis, *Neuroscience* **19**, 857 (1986).
- J. M. Bekkers and C. F. Stevens, *Nature* **346**, 724 (1990).
- R. Malinow and R. W. Tsien, *ibid.*, p. 177; S. J. Redman, *Physiol. Rev.* **70**, 165 (1990).
- I. D. Forsythe and G. L. Westbrook, *J. Physiol. London* **396**, 515 (1988); S. Hestrin, R. A. Nicoll, D. J. Perkel, P. Sah, *ibid.* **422**, 203 (1990); J. M. Bekkers and C. F. Stevens, *Nature* **341**, 230 (1989).
- R. A. J. Lester, J. D. Clements, G. L. Westbrook, C. E. Jahr, *Nature* **346**, 565 (1990); S. Hestrin, P. Sah, R. A. Nicoll, *Neuron* **5**, 247 (1990).
- C.-M. Tang, M. Dichter, M. Morad, *Science* **243**, 1474 (1989); L. O. Trussell and G. D. Fischbach, *Neuron* **3**, 209 (1989).
- R. H. Evans, A. A. Francis, J. C. Watkins, *Brain Res.* **148**, 536 (1979); H. McLennan and D. Lodge, *ibid.* **169**, 83 (1979).
- M. Benveniste and M. L. Mayer, *Br. J. Pharmacol.* **104**, 207 (1991).
- Hippocampal neurons from rats 1 to 3 days old were dissociated and grown in cell culture as described in (9). Whole-cell recordings were obtained with patch-clamp amplifiers (Warner Instruments, Hamden, CT) after the cells had been maintained for 1 to 2 weeks in culture. Currents were digitally sampled at 2 kHz and low-pass filtered at 1 kHz. Pipettes contained cesium gluconate, 150 mM (agonist-evoked currents) or potassium gluconate, 150 mM (EPSCs); NaCl, 10 mM; Hepes, 10 mM; and EGTA, 10 mM. Control extracellular solution contained NaCl, 155 mM; KCl, 3 mM; CaCl_2 , 2 mM; Hepes, 10 mM; D-glucose , 10 mM; glycine, 0.02 mM; and picrotoxin, 0.05 mM (pH 7.4). Reservoirs of media were connected to a series of glass flow pipes (400 μm inside diameter) by solenoid latching valves (General Valve, Fairfield, NJ) that were activated remotely by computer.
- Both pre- and postsynaptic neurons were voltage-clamped (-60 mV). A brief (1 to 2 ms) voltage step evoked an action potential in the axon of the presynaptic cell. Synaptic currents were evoked at 10-s intervals. Amplitudes were averaged over the range 20 to 100 ms after synaptic current onset. All solutions contained 6-cyano-7-nitroquinoxaline-2,3-dione (CNQX) ($2 \mu\text{M}$) to block AMPA receptor-mediated EPSCs.
- J. D. Clements and G. L. Westbrook, *Neuron* **7**, 605 (1991).
- M. Benveniste and M. L. Mayer, *Biophys. J.* **59**, 560 (1991).
- D. T. Monaghan, H. J. Olverman, L. Nguyen, J. C. Watkins, C. W. Cotman, *Proc. Natl. Acad. Sci. U.S.A.* **85**, 9836 (1988); K. H. Thedinger, M. S. Benedict, G. E. Fagg, *Neurosci. Lett.* **104**, 217 (1989).
- Currents were recorded (Axopatch 1B) from outside-out patches of hippocampal neuron membrane at a command potential of -50 mV . Ensemble averages were constructed from 20 to 100 trials. External solutions were gravity-fed to each lumen of four-barrel glass tubing (VitroDynamics, Rockaway, NJ) pulled to a final tip diameter of $\sim 200 \mu\text{m}$. Barrels were square and arranged in a square pattern. Solution changes (time constant $< 200 \mu\text{s}$) were effected by rapid movement of the interface between the solutions across the tip of the patch pipette with a piezoelectric translator (Physik Instrumente, Waldbronn, Germany, model P245.30). Control external solution contained NaCl, 180 mM; KCl, 2.5 mM; Hepes, 10 mM; glycine, 0.01 mM; picrotoxin, 0.02 mM; CNQX, 0.002 mM; and tetrodotoxin 0.0008 mM (pH 7.3). Internal solution contained CsCl, 150 mM; Hepes, 10 mM; and EGTA, 10 mM (pH 7.2).
- H. J. Olverman, A. W. Jones, J. C. Watkins, *Neuroscience* **26**, 1 (1988).
- R. H. Evans, A. A. Francis, K. Hunt, D. J. Oakes, J. C. Watkins, *Br. J. Pharmacol.* **67**, 591 (1979).
- A chemical kinetic model of D-AA and glutamate binding to the NMDA channel was constructed. The parameters of the model were adjusted to fit optimally the current transient recorded during exposure to 5 mM glutamate. The model and the optimization procedure for parameter estimation have been described in (22). Glutamate binding and unbinding rates as well as channel opening and closing rates were fixed at previously estimated values (15). The binding rate of D-AA was as determined in Fig. 2A. Only the D-AA unbinding rate, the desensitization and resensitization rates, and the number of channels contributing to the response were free variables in the optimization procedure.
- M. Benveniste, J. Clements, L. Vyklicky, Jr., M. L. Mayer, *J. Physiol. London* **428**, 333 (1990).
- The D-AA binding and unbinding rates of $8 \mu\text{M}^{-1} \text{ s}^{-1}$ and 160 s^{-1} , respectively, predict a microscopic K_d of $20 \mu\text{M}$, which is at the low end of the range of K_d values from whole-cell dose-response experiments (20 to $40 \mu\text{M}$). Because whole-cell K_d estimates rely on fewer assumptions and independent measurements than those from the kinetic approach, the D-AA binding and unbinding rates were adjusted ($7 \mu\text{M}^{-1} \text{ s}^{-1}$ and 210 s^{-1}) to give a K_d of $30 \mu\text{M}$. These rates were in the range from outside-out patches.
- A simulated "control response" to a synaptic pulse of glutamate was calculated. For each concentration of D-AA tested, we generated a simulated current by reducing the "control" EPSC amplitude by the same amount as the observed D-AA reduction of the EPSC. A simplex optimization procedure was used to estimate the transmitter concentration time course that best fitted the resulting family of simulated transients (that is, the time course that best explained the reduction in synaptic transmission caused by various concentrations of D-AA). The only free parameters in the optimization were the peak concentration of transmitter and the time constant of its exponential decay.
- J. M. Bekkers, G. B. Richerson, C. F. Stevens, *Proc. Natl. Acad. Sci. U.S.A.* **87**, 5359 (1990).
- D. Nicholls and D. Attwell, *Trends Pharmacol. Sci.* **11**, 462 (1990); P. M. Burger *et al.*, *Neuron* **3**, 715 (1989); N. Riveros, J. Fiedler, N. Lagos, C. Munoz, F. Orrego, *Brain Res.* **386**, 405 (1986).
- K. L. Magleby and C. F. Stevens, *J. Physiol. London* **223**, 173 (1972).
- D. Colquhoun, P. Jonas, B. Sakmann, *ibid.*, in press.
- D. K. Patneau and M. L. Mayer, *J. Neurosci.* **10**, 2385 (1990).
- H. C. Hartzell, S. W. Kuffler, D. Yoshikami, *J. Physiol. London* **251**, 427 (1975).
- We thank J. Volk for the preparation of cell cultures. Supported by U.S. Public Health Service grants NS21419 (C.E.J.), MH46613 (G.L.W.), and NS26494 (G.L.W.).

15 June 1992; accepted 13 August 1992